



## Evaluation of the Effects of Cross-Link Density and Swelling Ratio on Loading-Unloading Response in Large Strain Range of Hydrogels

メタデータ	言語: en 出版者: The Japanese Society for Experimental Mechanics 公開日: 2024-02-01 キーワード (Ja): キーワード (En): Hydrogel, Viscoelasticity, Swelling ratio, Cyclic deformation, Hyperelastic deformation 作成者: Morita, Syunpei, Uchida, Makoto, Kaneko, Yoshihisa, Okumura, Dai, Tanaka, Hiro, Ida, Shohei メールアドレス: 所属:
URL	<a href="http://hdl.handle.net/10466/0002000275">http://hdl.handle.net/10466/0002000275</a>

## Evaluation of the Effects of Cross-Link Density and Swelling Ratio on Loading-Unloading Response in Large Strain Range of Hydrogels

Syunpei MORITA<sup>1</sup>, Makoto UCHIDA<sup>1</sup>, Yoshihisa KANEKO<sup>1</sup>,  
Dai OKUMURA<sup>2</sup>, Hiro TANAKA<sup>3</sup> and Shohei IDA<sup>4</sup>

<sup>1</sup>Graduate School of Engineering, Osaka City University, Osaka 558-8585, Japan

<sup>2</sup>Department of Mechanical Systems Engineering, Nagoya University, Nagoya 464-8603, Japan

<sup>3</sup>Department of Mechanical Engineering, Osaka University, Suita 565-0871, Japan

<sup>4</sup>Faculty of Engineering, The University of Shiga Prefecture, Hikone 522-8533, Japan

(Received 11 February 2022; received in revised form 21 April 2022; accepted 23 April 2022)

**Abstract:** Hydrogel contains a large amount of solvent such as water inside a three-dimensional molecular chain network structure. The content of the solvent changes during the swelling and drying processes of the hydrogel. The mechanical properties of the gel significantly change depending on the solvent content. In this study, the effects of the cross-link density and swelling ratio on the nonlinear mechanical responses of hydrogel were investigated by the cyclic tensile test. To evaluate the irreversible deformation of the hydrogel, we performed the one-time and stepwise loading-unloading tests. The stress-strain curves for the loading and unloading process obtained from the crosshead displacement were different owing to the sliding between chuck and specimen. In contrast, they were consistent for all the experimental conditions when the strain was evaluated by the digital image correlation method. Therefore, the hydrogel showed the less-rate-dependent reversible deformation from small to large strain range. Furthermore, obtained results were compared with the theoretical model based on the molecular chain network model with swelling effect. Although the model could represent the nonlinear increase in the stress during the tensile test and the decrease in the stiffness owing to the swelling, the model results were not consistent with the experimental results. Experimental and numerical results indicate that the improvement of the mechanical model is necessary based on the less-rate-dependent reversible deformation mechanisms of the hydrogel.

**Keywords:** Hydrogel, Viscoelasticity, Swelling ratio, Cyclic deformation, Hyperelastic deformation

### 1. Introduction

The hydrogel is a soft polymer material with a three-dimensional molecular chain network structure, that contains a large amount of solvent such as water inside the network. Its mechanical properties change greatly depending on the solvent content. Currently, material development for hydrogel as a biomaterial is progressing in the fields of polymer chemistry and medicine [1]. It is known that the mechanical behavior of such materials strongly depends on the cross-link density and degree of swelling, and the effect of cross-link density on the swelling response has been investigated [2]. Mechanical-chemical models were developed to predict the changes in the mechanical properties during the swelling process [3-7].

To utilize the characteristics of hydrogels used in various applications, it is important to fully understand the mechanical properties of hydrogels. However, mechanical tests using flexible hydrogels cannot be performed in the mechanical tests similar to the hard materials. The main problem is that the contact type measurement method such as strain gauges and extensometers cannot be employed to measure the deformation of soft materials. Therefore, in this study, the strain of the gel specimen is measured using the digital image correlation (DIC), which is widely established as an effective optical method for measuring and evaluating the strain on the surface of the specimens.

So far, our research group has conducted uniaxial tensile tests of hydrogels with different swelling ratios and density of crosslinker and evaluated their mechanical properties using a molecular chain network model [8]. The comparison of stress-strain curves between experiment and simulation

showed a non-negligible mismatch. One of the possible reasons for the mismatch between the predicted and experimental results is that the gels generate an irreversible deformation due to tensile deformation and swelling.

In this paper, we evaluate the effects of the cross-link density and swelling ratio on the loading-unloading response in the large strain range of hydrogel specimens. The one-time and stepwise loading-unloading tensile tests are performed to evaluate the irreversible mechanical behavior of the hydrogel. Furthermore, obtained results are compared with the theoretical model based on the molecular chain network model with swelling effect.

### 2. Experimental Method

#### 2.1 Gel specimen

Table 1 shows the content of each constituent substance. In this experiment, acrylamide (AAm) was used as a monomer, and *N,N'*-methylenebisacrylamide (BIS) was used as a cross-linking agent. To evaluate the effect of the cross-link density, we prepared hydrogels with three different BIS contents, BIS 2.5, 5.0, 10.0. Ammonium persulfate (APS) and *N,N,N',N'*-tetramethylethylenediamine (TMEDA) were used as a polymerization initiators. First, the specified amount of AAm and BIS were measured by precision balance. Then, they were mixed in a beaker, and distilled water was added. Nitrogen gas was injected into the mixed solution to perform deoxidation treatment. Subsequently, polymerization was conducted using APS and TMEDA. The mixture was poured into a molded petri dish and covered with another small petri

Table 1 Components of gel

Specimen	BIS density [mM]	AAM [g]	BIS [mg]	APS [mg]	TMEDA [mL]	H <sub>2</sub> O [g]
BIS 2.5	2.5	3.73	5.775	17.1	0.0499	14.95
BIS 5.0	5.0	3.73	11.55	17.1	0.0499	14.95
BIS 10.0	10.0	3.73	23.10	17.1	0.0499	14.95

Table 2 Swelling Time and Swelling Ratio

	BIS2.5		BIS5.0		BIS10.0	
Swelling time [min]	20	1440	20	1440	20	1440
Swelling Ratio, $r_s$	1.595	3.103	1.516	2.865	1.424	2.216

dish. It was wrapped and left in the refrigerator for 2.5 hours with the weight on it.

As a specimen, a strip-shaped specimens with a length of 30 mm, a width of 10 mm, and a thickness of 1 mm were prepared. The obtained specimen is referred to as Specimen AP (As prepared). To evaluate the effect of the swelling ratio, the specimens were swollen in the distilled water at different times. Specimens with different swelling times, 20 min and 24 h are referred to as Specimen 20 min and 24 h, respectively. Because the solvent is non-uniformly distributed in the gel when the swelling time is short, the gel was retained in a nitrogen atmosphere for 60 minutes after swelling. The swelling ratio was defined as the ratio of the masses of swollen and AP hydrogels,  $m(t)/m_0$ . Table 2 shows the swelling ratio of each specimen.

### 2.2 Experimental procedure

To investigate the effects of the strain history on the irreversible deformation of the hydrogel, the loading-unloading tensile tests of the hydrogel specimens with different swelling ratios were performed. As shown in Fig. 1, we performed the one-time and stepwise loading-unloading tests. In the one-time test, the single loading-unloading process within the testing deformation range was given to the hydrogel specimen, whereas the repetitive loading-unloading process within the stepwisely increasing testing deformation ranges was given to the hydrogel specimen in the stepwise test.

The effect of the applied strain on the irreversible strain of the hydrogel can be evaluated by comparing the results obtained from both experiments. A loading-unloading process within the tensile displacement from 0 mm to 20 mm was given to the hydrogel specimen with the initial length of 15 mm in the one-time loading-unloading test. By contrast, the repetitive loading-unloading process with the maximum tensile displacements of 5 mm, 10 mm, 15 mm, and 20 mm were given to the hydrogel specimen in the stepwise loading-unloading test.

Subsequently, to investigate the effects of cross-link density and swelling ratio on the irreversible deformation of the hydrogel, we performed the one-time loading-unloading tensile tests of hydrogel specimens with different BIS contents and swelling time. In this test, different degrees of strain were given to the specimen because the fracture strain depends on the BIS contents. 1.25, 0.75, and 0.5 of true strain estimated by the crosshead displacement were applied to the specimens with BIS2, 5, and 10, respectively.

Figure 2(a) shows the experimental setup. The automatic vertical servo stand (JSVH1000, Nippon Measurement

System Co., Ltd.) was used in the cyclic and loading-unloading tests. To reduce the slippage of the gel specimen, Styrofoam adhered to the chuck surface. As experimental conditions, the initial distance between jigs was set at 15 mm, and the tensile speed was set at 15 mm/min. Since DIC was employed in this experiment, sequential images of the specimen surface were taken every 4 sec.

### 2.3 Strain evaluation of deformation

#### 2.3.1 NetDIC

The displacement of the measurement points is evaluated using netDIC [9]. In the conventional DIC, a subset of the brightness map is defined around the object point (point of interest, POI) to evaluate the displacement of the POI in Fig. 2(b). Then, corresponding points between images obtained before and after time increment are obtained when the correlation between their brightness maps is maximized. In the netDIC, the deformation of the subset for the POI is approximated using displacements of other measurement points around the POI. Therefore, the continuity of the deformation around the POI is introduced in this method, thereby enabling a stable displacement evaluation under the prominent nonuniform deformation, such as the neck propagation process in the case of polymers [9,10].

#### 2.3.2 Evaluation of true stress and true strain

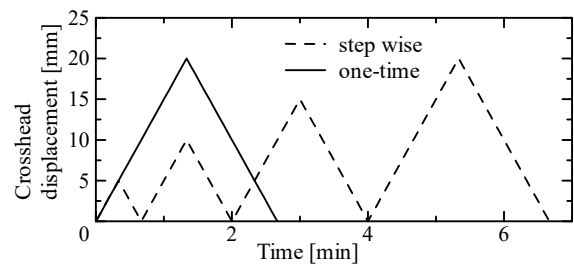
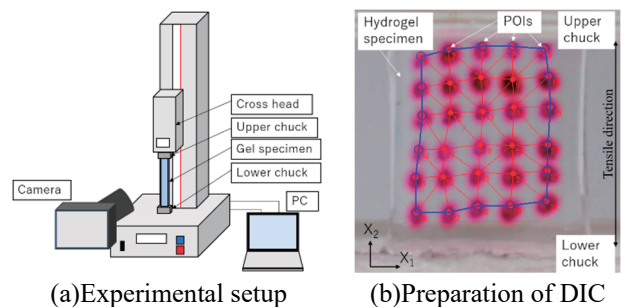


Fig. 1 Crosshead displacement for one-time and stepwise loading-unloading tests.



(a) Experimental setup (b) Preparation of DIC

Fig. 2 Experimental methods for tests.

Because the measurement method using extensometer or strain gauge cannot be employed for the hydrogel, true strain and true stress were estimated using the crosshead displacement  $u_{CH}$ . The true strain  $\varepsilon_{CH}$  and true stress  $\sigma_{CH}$  estimated using  $u_{CH}$  are

$$\varepsilon_{CH} = \ln \left( 1 + \frac{u_{CH}}{L_0} \right) \quad (1)$$

$$\sigma_{CH} = \frac{F}{A_0} \left( 1 + \frac{u_{CH}}{L_0} \right) \quad (2)$$

where,  $L_0$  is the initial distance between the upper chuck and the lower chuck,  $A_0$  the initial cross-section,  $F$  tensile force, respectively.

However, the non-uniform deformation in the hydrogel and the sliding between chuck and hydrogel may affect the strain measurement when the crosshead displacement was used. Therefore, we evaluated the strain field on the hydrogel specimen surface by DIC. After acquiring the displacement of the measurement point, the strain field is evaluated. The triangular elements are constructed using the displacement-measurement points based on the Delaunay triangulation scheme. The deformation gradient tensor of the triangular element is calculated using displacement vectors on the vertex of the triangle as shown in Fig. 3.

The deformation gradient is given by the following equation:

$$F = \frac{\partial \mathbf{x}}{\partial \mathbf{X}} = \mathbf{I} + \frac{\partial \mathbf{u}}{\partial \mathbf{X}} \quad (3)$$

where,  $\mathbf{X}$  and  $\mathbf{x}$  are the coordinates before and after the deformation,  $\mathbf{u} = \mathbf{x} - \mathbf{X}$  is the displacement vector, and  $\mathbf{I}$  is the unit tensor.

The two-dimensional component of the displacement gradient  $\partial \mathbf{u} / \partial \mathbf{X}$  of the triangular element composed of the contact points of the triangular element ( $P^{(1)}$   $P^{(2)}$   $P^{(3)}$ ) is given in vector form.

$$\begin{Bmatrix} \partial u_1 / \partial X_1 \\ \partial u_2 / \partial X_2 \\ \partial u_1 / \partial X_2 \\ \partial u_2 / \partial X_1 \end{Bmatrix} = \frac{1}{2\Delta} [\mathbf{A}] \begin{Bmatrix} u_1^{(1)} \\ u_2^{(1)} \\ u_1^{(2)} \\ u_2^{(2)} \\ u_1^{(3)} \\ u_2^{(3)} \end{Bmatrix} \quad (4)$$

where,

$$[\mathbf{A}] = \begin{bmatrix} X_2^{(2)} - X_2^{(3)} & 0 & X_2^{(3)} - X_2^{(1)} & 0 & X_2^{(1)} - X_2^{(2)} & 0 \\ 0 & X_1^{(2)} - X_1^{(3)} & 0 & X_1^{(3)} - X_1^{(1)} & 0 & X_1^{(1)} - X_1^{(2)} \\ X_1^{(2)} - X_1^{(3)} & 0 & X_1^{(3)} - X_1^{(1)} & 0 & X_1^{(1)} - X_1^{(2)} & 0 \\ 0 & X_2^{(2)} - X_2^{(3)} & 0 & X_2^{(3)} - X_2^{(1)} & 0 & X_2^{(1)} - X_2^{(2)} \end{bmatrix}$$

$u_i^{(N)}$  and  $X_i^{(N)}$  are vectors of the displacement and reference coordinate for  $N$  the vertex of the element, and  $\Delta$  represents the area of the triangular element, respectively.

Left Cauchy-Green Tensor  $\mathbf{V}$  is given by the following equation.

$$\mathbf{V}^2 = \mathbf{F} \cdot \mathbf{F}^T \quad (5)$$

Therefore, the local true strain tensor  $\boldsymbol{\varepsilon}$  is given by the following equation.

$$\boldsymbol{\varepsilon} = \ln \mathbf{V} \quad (6)$$

The overall true strain  $\varepsilon_{DIC}$  and true stress  $\sigma_{DIC}$  in the loading direction were evaluated by the following equations.

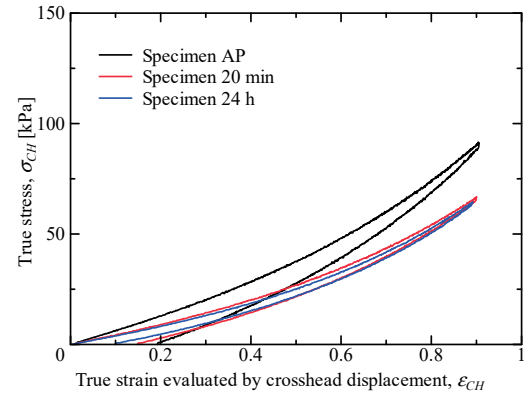
$$\varepsilon_{DIC} = \frac{1}{V} \int_V \varepsilon_{22} dV \quad (7)$$

$$\sigma_{DIC} = \frac{F}{A_0} \exp(\bar{\varepsilon}_{22}) \quad (8)$$

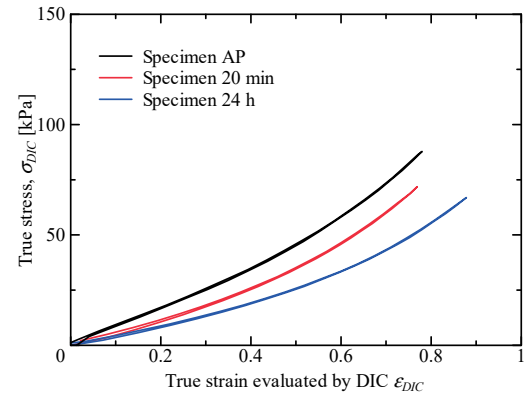
where  $V$  is the volume of the displacement evaluation region.

### 3. Results

First, Fig.3 shows the relationships between true stress and true strain for the one-time loading-unloading test for the hydrogel specimens with different swelling ratios. True stress and strain in Fig. 3 (a) and (b) were estimated by crosshead displacement and DIC, respectively. In Fig. 3 (a), the loading and unloading processes are different, and the residual strain is observed after unloading. In contrast, the loading and unloading processes are almost the same in Fig. 3 (b). Although the stress becomes lower with the increasing



(a) Strain estimated by crosshead displacement



(b) Strain estimated by DIC

Fig. 3 Relationships between true stress and true strain under one-time loading-unloading test.

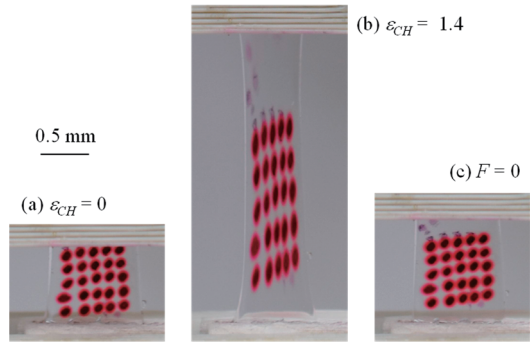


Fig. 4 Images of Specimen AP at (a) before tensile test, (b) after loading, and (c) after unloading processes.

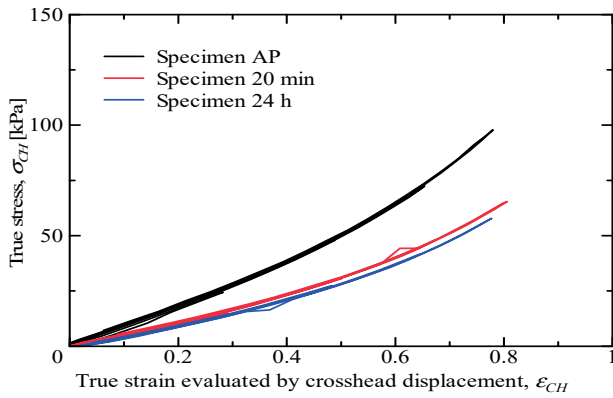


Fig. 5 Relationships between true stress  $\sigma_{DIC}$ -true strain  $\epsilon_{DIC}$  for stepwise loading-unloading test

swelling ratio, the residual strain is not observed for all the swelling conditions. Therefore, the results obtained by crosshead displacement include the pseudo strain caused by the sliding between chuck and specimen.

Figure 4 shows pictures of the specimen AP (a) before deformation ( $\epsilon_{CH} = 0$ ), (b) after loading ( $\epsilon_{CH} = 1.4$ ) and (c) after unloading ( $F = 0$ ) of one-time loading-unloading

test, respectively. The red circles on the specimen are the reference marker for the DIC measurement. We can see that the upper and lower margins, in which the red circles are not given, expand after loading, and it remains after unloading. These results clearly showed that sliding occurs when the tensile load was applied to the hydrogel specimen. Because this pseudo residual strain was observed for all the conditions of the tensile test, the strain estimated by the crosshead displacement cannot be used for the evaluation of the irreversible strain of the hydrogel.

Figure 5 shows the true stress-true strain curves evaluated by DIC for the stepwise loading-unloading test. As well as the one-time loading-unloading test, the residual strain is not observed even when the repetitive loading-unloading cycles are applied to the hydrogel specimen. The consistency of the loading and unloading processes also indicated the viscous strain which causes the change in the stress-strain curve is quite small in the hydrogel from small to large strain range. The decrease in the viscosity by swelling was also observed in references [12-14]. The viscosity is an important characteristic of the polymer. Although the degree of the viscous strain cannot be evaluated in this study, the viscous property of the swollen hydrogel will be characterized by an accurate measurement such as DMA in the future study.

Next, the effect of the cross-link density on the loading-unloading process is investigated. Figure 6 shows the development of distribution of the true strain in loading direction during the loading-unloading test. Figures 6 (a) and (b) are results for specimens AP and 24h, respectively. We can observe that uniform deformation occurs for all specimens under the uniaxial tensile test. The important result is that the specimen shapes and strain distributions before and after the loading-unloading test are almost the same. Figure 7 shows the relationships between true stress and true strain under one-time loading-unloading test for specimens (a) BIS 2.5 and (b) BIS 10.0, respectively. With

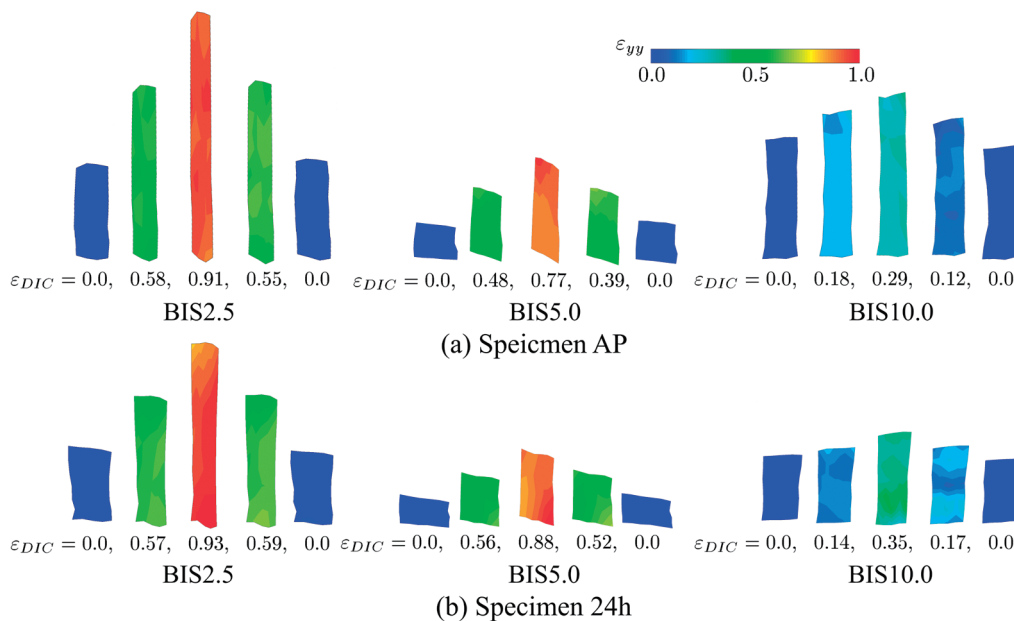


Fig. 6 Distribution of strain in loading direction under loading-unloading test.

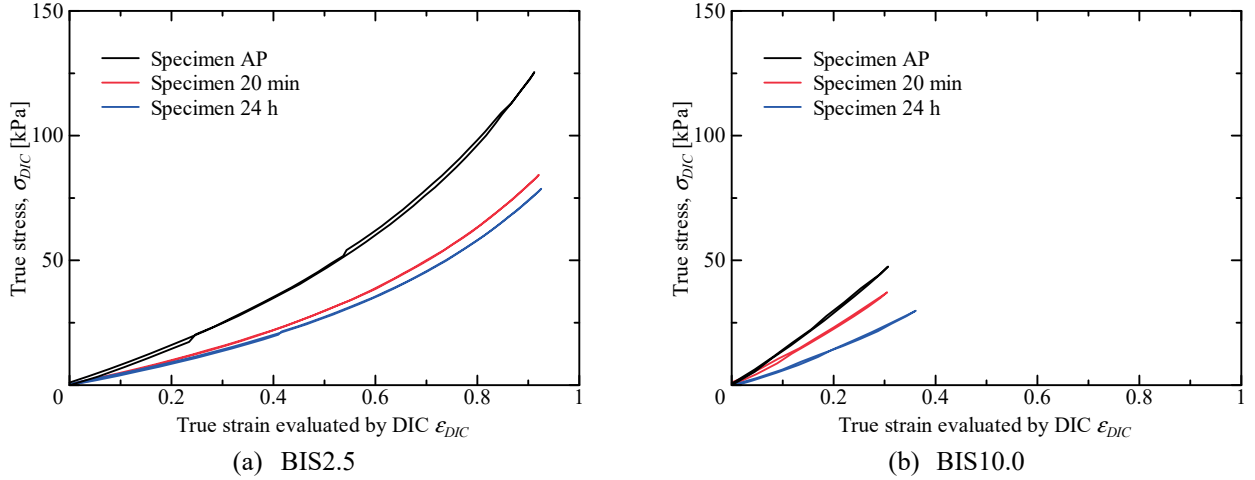


Fig. 7 Relationships between true stress  $\sigma_{DIC}$  and true strain  $\varepsilon_{DIC}$  under one-time loading-unloading test of hydrogel specimens with different BIS contents.

increasing BIS contents, the initial elastic modulus increases, and the elongation decreases. However, the irreversible deformation cannot be observed for all specimens with different BIS contents and swelling ratios.

The irreversible deformation of polymeric material is induced by weak interaction such as van der Waals bonding between adjacent molecular chains in the polymer network. Because the distance between molecular chains decreases for hydrogel with higher polymer density, the irreversible deformation may occur by intermolecular bonding. However, such an irreversible response was not observed in the hydrogels prepared in this study. The existence of the solvent in the polymer network may expand the distance between adjacent molecular chains. Therefore, the irreversible deformation caused by the interaction between adjacent molecular chains may not occur in the hydrogel. Furthermore, the stress caused by the reversible deformation may be significantly larger than that caused by the irreversible deformation. the irreversible deformation may be observed when the hydrogel with quite a lower cross-link density is employed for the loading-unloading test.

The deformation of polymers above the glass transition temperature  $T_g$  is typically modeled by the entropic elasticity. The glass transition temperature  $T_g$  of dried hydrogel is 165 °C [15]. However,  $T_g$  rapidly decreases owing to the content of the solvent [16]. Although  $T_g$  of employed hydrogels, which contains at least approximately 80 wt% of solvent, was not measured, the monotonically increasing stress-strain curves indicate that the employed hydrogels were in the rubbery state at room temperature. Therefore, using the entropic elasticity model in which the swelling effect is introduced, we discuss the effects of the cross-link density and swelling ratio on the true stress-strain response of the hydrogel. Based on the three-dimensional polymer network model proposed by Arruda and Boyce [11], the relationship between true stress  $\sigma$  and stretch  $\lambda$  under uniaxial tensile stress can be expressed as

$$\sigma = \frac{1}{3} C_R \frac{\sqrt{N}}{\lambda_c} \mathcal{L}^{-1} \left( \frac{\lambda_c}{\sqrt{N}} \right) \left( \lambda^2 - \frac{1}{\lambda} \right), \quad (9)$$

where  $C_R$  is the rubbery modulus,  $N$  is the number of segments per molecular chain,  $\lambda_c = \left\{ (\lambda^2 + 1/\lambda) / 3 \right\}^{1/2}$  is the molecular chain stretch, and  $\mathcal{L}^{-1}(x)$  is the inverse function of the Langevin function.

Here we assumed that the stretch of hydrogel,  $\lambda$ , is decomposed into that caused by swelling,  $\lambda_s$ , and that caused by external loading,  $\lambda_e$ , as  $\lambda = \lambda_e \lambda_s$ . Furthermore, because the rubbery modulus  $C_R$  is proportional to the chain density,  $C_R$  decreased by swelling as  $C_R' = \lambda^{-3} C_R$ . Finally, the constitutive equation for swollen hydrogel under the uniaxial test is given by

$$\sigma = \frac{1}{3} C_R \frac{\sqrt{N}}{\lambda_s \lambda_{ec}} \mathcal{L}^{-1} \left( \frac{\lambda_s \lambda_{ec}}{\sqrt{N}} \right) \left( \frac{\lambda_e^2}{\lambda_s} - \frac{1}{\lambda_s \lambda_e} \right), \quad (10)$$

where  $\lambda_{ec} = \lambda_c / \lambda_s$ . The material's parameters,  $C_R$  and  $N$ , which were obtained from experimental data by the least square method, were shown in Table 3. The rubbery modulus  $C_R$  increases and the segment number per chain  $N$  decreases with increasing BIS contents, respectively.

The comparison of true stress-strain response obtained from the experiment and model for all the conditions are shown in Fig. 8. Because the swelling stretch is isotropic,  $\lambda_s$  is given by  $\lambda_s = r_s^{1/3}$ , where  $r_s$  is the swelling ratio in Table 2. To compare the responses, the deformation caused by the swelling,  $\lambda_s$ , is removed in this graph. Therefore, the true strain for the model is calculated by  $\varepsilon = \ln \lambda_e$ . The model can represent the nonlinear increase in the stress during the tensile test and the decrease in the stiffness owing to the swelling. However, the model result is not consistent with the experimental results. The model underestimates the degree of stress decrease owing to the swelling. Experimental and numerical results indicate that the improvement of the mechanical model is required based on the less-rate-dependent reversible deformation mechanisms of the hydrogel.

One of the possible deformation mechanisms is that the molecular chain density reversibly changes during stretching. The intermolecular bonds can be divided into chemical cross-linking and physical entanglement. Some of

Table 3 Material parameters

	BIS2.5	BIS5.0	BIS10.0
$C^R$ [MPa]	19.0	18.9	35.9
$N$	105.0	84.3	58.8

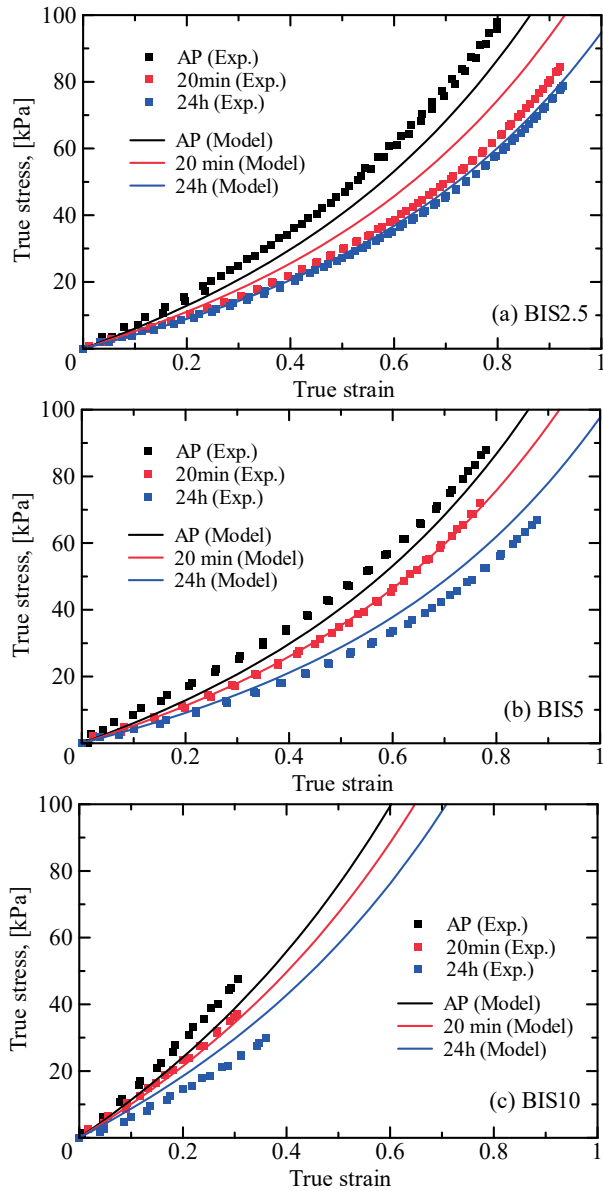


Fig. 8 Comparison of relationships between true stress and true strain for experiment and model

the physical entanglement may decrease and increase owing to external loading or deformation caused by swelling, which results in changes in molecular chain density and strength. The other is the generation of residual stress owing to swelling. When the solvent is contained in the polymer network, the molecular chain is stretched. This may induce residual stress in the molecular chains, which changes the deformation behavior in the response to further stretching. The mechanical model of hydrogel will be updated based on experiments with wider ranges of loading conditions and material profiles in the future study.

#### 4. Conclusion

In this study, the effects of the cross-link density and swelling ratio on the nonlinear mechanical behavior of hydrogels were investigated by one-time and stepwise loading-unloading tests, and the irreversible deformation of hydrogels was discussed.

The stress-strain curves for the loading and unloading process obtained from the crosshead displacement were different, and the residual strain was observed owing to the sliding between chuck and specimen. In contrast, they were consistent for all the experimental conditions when the strain was evaluated by DIC. Therefore, the hydrogel showed the less-rate-dependent reversible deformation from small to large strain range.

The strength of the hydrogel is higher for those with higher cross-link densities and lower swelling ratios. To represent these experimental results, the theoretical model based on the molecular chain network model with swelling effect was employed. Although the model could represent the nonlinear increase in the stress during the tensile test and the decrease in the stiffness owing to the swelling, the model underestimated the degree of stress decrease owing to the swelling. Experimental and numerical results indicate that the improvement of the mechanical model is necessary based on the less-rate-dependent reversible deformation mechanisms of the hydrogel.

#### Acknowledgement

The authors gratefully acknowledge a Grant-in-Aid for Scientific Research(A)(JSPS KAKENHI grant number 19H00739) from the Japan Society for the Promotion of Science.

#### References

- [1] Drozdov A.D. and Christiansen J. C.: Double-network gels with dynamic bonds under multi-cycle deformation, *Journal of the Mechanical Behavior of Biomedical Materials*, **88**(2018), 58–68.
- [2] Eichenbau, G. M., Kiser, P. F., Dobrynin, A. V., Simon, S. A. and Needham, D.: Investigation of the swelling response and loading of ionic microgels with drugs and proteins: the dependence on cross-link density, *Macromolecule.*, **32**(1999),4867–4878
- [3] Flory, P. J. and Rehner, J.: Statistical mechanics of cross - linked polymer networks I. rubberlike elasticity, *The Journal of Chemical Physics*, **11**(1943), 521–526.
- [4] Chester, S. A. and Anand, L.: A coupled theory of fluid permeation and large deformations for elastomeric materials, *Journal of the Mechanics and Physics of Solids*, **58**(2010), 1879–1906.
- [5] Okumura, D., Kondo A. and Ohno, N.: Using two scaling exponents to describe the mechanical properties of swollen elastomers, *Journal of the Mechanics and Physics of Solids*, **90**(2016), 61–76.
- [6] Okumura, D., Mizutani, M. Tanaka, H. and Uchida, M.: Effects of two scaling exponents on biaxial deformation and mass transport of swollen elastomers, *International Journal of Mechanical Sciences*, **146-147**(2018),507–516.

- [7] Okumura, D. and Chester, S. A.: Ultimate swelling described by limiting chain extensibility of swollen elastomers, *International Journal of Mechanical Sciences*, **144**(2018), 531–539.
- [8] Uchida, M., Sengoku, T., Kaneko, Y., Okuda, D., Tanaka, H. and Ida, S.: Evaluation of the effects of cross-linking and swelling on the mechanical behaviors of hydrogels using the digital image correlation method, *Softmatter*, **15**(2019), 3389–3396.
- [9] Uchida, M. and Tada, N.: Sequential evaluation of continuous deformation field of semi-crystalline polymers during tensile deformation accompanied by neck propagation, *International Journal of Plasticity*, **27**(2011), 2085–2102
- [10] Uchida, M., Tanaka, S., Kanagawa, T. and Tada, N.: Three-dimensional evaluation of strain field during neck propagation process of semi-crystalline polymer by time-series net DIC, *Transactions of the JSME*, **A78**–792(2012), 1133–1145
- [11] Arruda, E. M. and Boyce, M. C.: A three-dimensional constitutive model for the large stretch behavior of rubber elastic materials, *Journal of the Mechanics and Physics of Solids*, **41**(1993), 389–421.
- [12] Grattoni, C. A., Al-Sharji, H. H., Yang, C., Muggeridge, A. H. and Zimmerman, R. W.: Rheology and permeability of crosslinked polyacrylamide gel, *Journal of Colloid and Interface Science*, **240** (2001), 601–607.
- [13] Savart, T., Dove, C. and Love, B. J.: In situ dynamic rheology study of polyacrylamide during gelation coupled with mathematical models of viscosity advancement, *Macromolecular Materials and Engineering*, **295** (2010), 146–152.
- [14] Bosnjak, N., Nadimpalli, S., Okumura, D. and Chester, S. A.: Experiments and modeling of the viscoelastic behavior of polymeric gels, *Journal of the Mechanics and Physics of Solids*, **137** (2019), 103829 (22p.).
- [15] Brandrup, J., Immergut, E. H. and Grulke, E. A.: *Polymer Handbook* (4th ed.), Wiley (2003).
- [16] Pissis, P. and Kyritsis, A.: Hydration studies in polymer hydrogels, *Journal of Polymer Science, Part B, Polymer Physics*, **51** (2013), 159–175.